

THREE-DIMENSIONAL HYDROMAGNETIC CONVECTIVE FLOW OF CHEMICALLY REACTIVE EYRING-POWELL FLUID WITH NON- UNIFORM HEAT SOURCE/SINK

L. Padmavathi¹

¹Assistant Professor, Department of Mathematics, Sai Rajeswari Institute of Technology,
Proddatur-516360, A.P, India.

ABSTRACT

The three-dimensional hydromagnetic flow of an Eyring-Powell non-Newtonian fluid on a bilinear stretching sheet embedded porous medium has been considered to investigate the thermal radiation, non-uniform heat source/sink and first ordered chemical reaction. The corresponding non-linear partial differential equations (PDE's) are transmuted into set of ordinary differential equations (ODE's) by means of similarity transformations. The resulting coupled non-linear equations are evaluated numerically by employing boundary value problem default solver in MATLAB bvp4c package. Pertinent results are graphically represented in the analysis of various physical parameters of velocity, temperature and concentration distributions. Moreover, the numerical values of skin-friction factor, rate of heat and mass transfers are tabulated. It is found that the axial and transverse velocities are depreciated by Eyring-Powell fluid parameter, while an opposite tendency encountered in temperature and concentration fields.

Key words: Three-dimensional flow, Hydromagnetic, Eyring-Powell fluid, Non-uniform heat source/sink, Soret effect.

1. INTRODUCTION

The study of boundary layer flow over a stretching sheet has generated much interest in recent years in view of its numerous industrial applications such as the aerodynamic extrusion of plastic sheets, the boundary layer along a liquid film, condensation process of metallic plate in a cooling bath and glass, and also polymer industries. The mechanical properties of the final product strictly depend on the stretching and cooling rates in the process. Patel et al. [1] reported that the Eyring-Powell model is useful and has significant benefits in comparison with the power law model. Fluid flow close to a dynamic plate for the Eyring-Powell with the help of three different techniques. Hayat et al. [2] explored the radiative effects on the three-dimensional magnetohydrodynamic (MHD) flow of an Eyring-Powell fluid. Moreover, Ara et al. [3] have studied the Eyring-Powell fluid under the thermal radiation effect over an exponentially shrinking sheet. Javed et al. [4] studied the boundary layer flow over a stretching sheet for non-Newtonian fluid, namely the Eyring-Powell model. Nadeem et al. [5] However, to the best of our knowledge no attempt has been made to study Eyring-Powell fluid over an exponentially shrinking sheet. Hayat et al. [6] studied the steady flow of an Powell-Eyring fluid over a moving surface with convective boundary conditions. Rosca et al. [7] is studied the flow and heat transfer of Powell-Eyring fluid over shrinking surface in a parallel free stream. Jalil et al. [8] studied the flow and heat transfer of Powell-Eyring fluid over a moving surface in a parallel free stream.

In recent times, knowledge in boundary layer flow with heat and mass transfer is paying attention to researchers because of its several important applications. In particular, the combined effect of heat and mass transfer plays a vital role in numerous engineering applications. Many researchers are inspired and still engaged with the discussion of heat and mass transfer effects in the flow over a stretching surface. Magyari et al. [9] studied the heat and mass characteristics of boundary layer flow. Chen [10] discussed the influence of frictional and Ohmic heating on MHD flow of Newtonian liquid past a vertical surface. Sagar et al. [11] studied the heat and mass transport effects on natural convective flow of non-Newtonian fluid with magnetic field. Patel et al. [12] numerically examined the flow of Powell-Eyring model through asymptotic boundary conditions. Gireesha et al. [13] studied boundary layer flow and heat transfer of a dusty fluid over an exponentially stretching sheet. Mukhopadhyay et al. [14] investigated the slip effects on MHD boundary layer flow by an exponentially stretching sheet with suction/blowing and thermal radiation. Al-Odat et al. [15] studied thermal boundary layer on an exponentially stretching continuous surface in the presence of magnetic field. Malik et al. [16] presented boundary layer flow of an Eyring-Powell model fluid due to a stretching cylinder with variable viscosity. Nabil et al. [17] studied numerical study of viscous dissipation effect on free convection heat and mass transfer of MHD Eyring-Powell fluid flow through a porous medium. Rubab et al. [18] studied cattaneo-christov heat flux model for MHD three Dimensional flow of maxwell fluid over a stretching sheet. Murshed et al. [19] discussed about a review of boiling and convective heat transfer with nanofluids.

Magnetohydrodynamics is combination of electrically conducting fluids and magnetic fields, MHD flows occur in the ionosphere, sun, power generators, etc. Hydromagnetic effects play a vital role in the study of non-Newtonian fluids. The following are a few investigations about electrically conducting non-Newtonian Eyring-Powell fluids. Najeeb et al. [20] discussed Eyring-Powell fluid on a rotating disk with the influence of a transverse magnetic field and they observed that the fluid velocity reduced in all directions with the influence of a magnetic field. Malik et al. [21] investigated the mixed convection flow of hydromagnetic Eyring-Powell nanofluid on a stretching sheet and they noticed that the magnetic field decreases the skin friction. Mahanthesh et al. [22] illustrated the magnetohydrodynamic effects on nano Eyring-Powell fluid over a stretching sheet and they concluded that the applied magnetic field reduces the velocity profile. Hayat et al. [23] evaluated the hydromagnetic fluid flow of Powell-Eyring nano-material over a nonlinearly stretching sheet and they found that the fluid temperature and concentration enriched with increasing magnetic field parameters. Hayat et al. [24] examined the electrically conducting flow of Powell-Eyring nanofluid on a stretching cylinder and they stated that the skin friction enhanced with Hartmann number and curvature parameter.

The non-Newtonian fluids have played a very significant role in technical and engineering fields. Various rheological relations have been recommended in order to investigate the flow and heat transfer properties among them the Eyring-Powell fluid model is one of these non-Newtonian models. This kind of fluid model is complex in nature but has some aspects instead of other fluids. Han et al. [25] studied coupled flow and heat transfer in viscoelastic fluid with the Cattaneo-Christov heat flux model. Hayat et al. [26] considered the heat and mass flux boundary conditions for the analysis of three-dimensional flow of Eyring-Powell nanofluid and they concluded that the thermal radiation enhances the thickness of the thermal boundary layer and rate of heat transfer. Rahimi et al. [27] described the Solution of the boundary layer flow of an Eyring-Powell non-Newtonian fluid over a linear stretching sheet by the collocation method. Geethan kumar et al. [28] studied Diffusion-Thermo effect on three-dimensional conducting flow of Eyring-Powell fluid over a bilinear stretching porous sheet with chemical reaction and diffusion Slip. Ishak et al. [29] studied MHD stagnation point flow towards a stretching sheet. The influence of heat generation and absorptions on the porous flow of Eyring-Powell fluid on the unsteady oscillatory stretching sheet was investigated by Dawar et al. [30] and they found that the rate of heat transfer increased with the increasing values of thermal radiation parameter and Prandtl number while it reduced with porosity parameter. Gbadeyan et al. [31] analyzed the Soret and Dufour effects on the hydrodynamic mixed convective flow of viscoelastic fluid through a vertical stretching surface filled with porous medium, and they observed that the increasing of thermal boundary layer thickness and decreasing of heat transfer with increasing values of Dufour number. Khan et al. [32] performed an investigation on the effect of entropy generation in the steady and axisymmetric flow of an incompressible Powell-Eyring fluid with Dufour and Soret effects. Suali et al. [33] analyzed unsteady stagnation point flow and heat transfer over a stretching/shrinking sheet with prescribed surface heat flux. Zaman et al. [34] presented unsteady incompressible Couette flow problem for the Eyring-Powell model with porous walls. Hayat et al. [35] investigated the three-dimensional flow of Powell-Eyring nanofluid with heat and mass flux boundary conditions. By the stimulation of the above studies, this paper chapter investigates three-dimensional hydromagnetic non-Newtonian fluid flows. So, in this study, we investigated the three-dimensional hydromagnetic flow of non-Newtonian Eyring-Powell fluid through a bilinear stretching sheet embedded in a porous medium with thermal radiation, non-uniform heat source or sink and first ordered destructive chemical reaction. With the help of self-similar transformations, the set of partial differential equations is transformed into the set of ordinary differential equations and they are evaluated by numerical method along with MATLAB bvp4c by Shooting technique.

2. MATHEMATICAL FORMULATION

The three-dimensional flow of Eyring-Powell fluid over a bilinear stretching sheet with porous medium is considered for investigation of different fluid flow characteristics. The sheet is considered along xy -plane (i.e., $z = 0$) and linearly stretched with the stretching velocities $U_w = ax$ and $V_w = by$ in x and y directions, respectively (where a and b are stretching constants). The electrical and induced magnetic fields are neglected due to consideration of small magnetic Reynolds number and the applied magnetic field B_0 is taken normal to the flow direction. The thermal radiation, non-uniform heat source or sink, Soret effect, and first order destructive chemical reaction effects are taken into account. The effect of Hall current is neglected. The physical model and coordinate system for the above considerations are pictured in fig.6.1.

The rheological model for the Eyring-Powell fluid model taken as:

$$\tau_{ij} = \mu \frac{\partial u_i}{\partial x_j} + \frac{1}{\beta} \sinh^{-1} \left(\frac{1}{c} \frac{\partial u_i}{\partial x_j} \right)$$

$$\sinh^{-1} \left(\frac{1}{c} \frac{\partial u_i}{\partial x_j} \right) \cong \frac{1}{c} \frac{\partial u_i}{\partial x_j} - \frac{1}{6} \left(\frac{1}{c} \frac{\partial u_i}{\partial x_j} \right)^3, \left| \frac{1}{c} \frac{\partial u_i}{\partial x_j} \right| \ll 1$$

Here β and c are Eyring-Powell fluid characteristics.

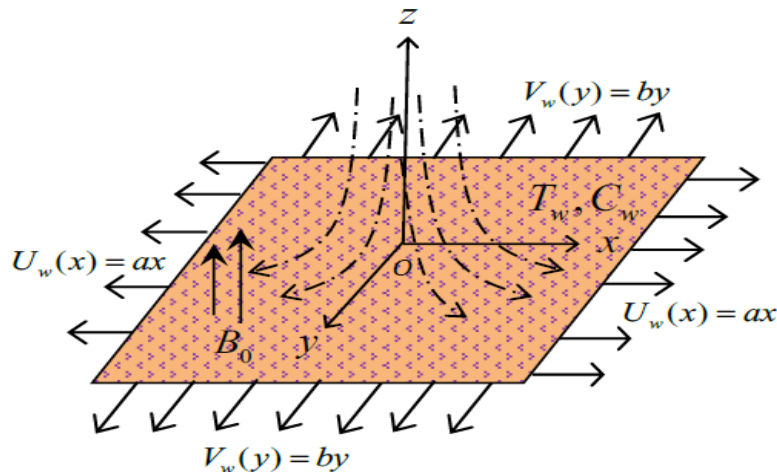


Fig.2.1 Physical model and coordinate system.

According to the above assumptions, the governing equations are constructed as follows:

$$\frac{\partial u}{\partial x} + \frac{\partial v}{\partial y} + \frac{\partial w}{\partial z} = 0 \quad (1)$$

$$\left(u \frac{\partial u}{\partial x} + v \frac{\partial u}{\partial y} + w \frac{\partial u}{\partial z} \right) = \left(\nu + \frac{1}{\rho\beta c} \right) \frac{\partial^2 u}{\partial z^2} - \frac{1}{2\rho\beta c} \left(\frac{\partial u}{\partial z} \right)^2 \frac{\partial^2 u}{\partial z^2} - \left(\frac{\sigma B_0^2}{\rho} + \frac{\nu}{k_p} \right) u \quad (2)$$

$$\left(u \frac{\partial v}{\partial x} + v \frac{\partial v}{\partial y} + w \frac{\partial v}{\partial z} \right) = \left(\nu + \frac{1}{\rho\beta c} \right) \frac{\partial^2 v}{\partial z^2} - \frac{1}{2\rho\beta c} \left(\frac{\partial v}{\partial z} \right)^2 \frac{\partial^2 v}{\partial z^2} - \left(\frac{\sigma B_0^2}{\rho} + \frac{\nu}{k_p} \right) v \quad (3)$$

$$u \frac{\partial T}{\partial x} + v \frac{\partial T}{\partial y} + w \frac{\partial T}{\partial z} = \frac{\kappa}{\rho C_p} \frac{\partial^2 T}{\partial z^2} - \frac{1}{\rho C_p} \frac{\partial q_r}{\partial z} + \frac{q'''}{\rho C_p} \quad (4)$$

$$u \frac{\partial C}{\partial x} + v \frac{\partial C}{\partial y} + w \frac{\partial C}{\partial z} = D \frac{\partial^2 C}{\partial z^2} - k_1 (C - C_\infty) \quad (5)$$

The radiative heat flux q_r is given by

$$q_r = \frac{-4\sigma^* \partial T^4}{3k^* \partial z} \quad (6)$$

Where k^* is the mean absorption coefficient, σ^* is the Stefan-Boltzmann constant and the linear temperature function T^4 is expanded by using Taylors series expansion in terms of T_∞ as

$$T^4 = 4T_\infty^3 T - 3T_\infty^4 \quad (7)$$

Thus substituting Eq. (1.7) in Eq. (1.6), we get

$$q_r = -\frac{16\sigma^* T_\infty^3}{3k^*} \frac{\partial T}{\partial z} \quad (8)$$

The non-uniform heat source/sink, q''' , is defined as

$$q''' = \frac{kU_w}{\nu x} [A^* (T_w - T_\infty) f' + B^* (T - T_\infty)] \quad (9)$$

Where, A^* and B^* are the coefficients of space dependent and temperature dependent heat source/sink, respectively. The case $A^* > 0, B^* > 0$ corresponds to internal heat source and the case $A^* < 0, B^* < 0$ corresponds to internal heat sink.

Then the heat transfer equation becomes

$$u \frac{\partial T}{\partial x} + v \frac{\partial T}{\partial y} + w \frac{\partial T}{\partial z} = \frac{\kappa}{\rho C_p} \frac{\partial^2 T}{\partial z^2} + \frac{16\sigma^* T_\infty^3}{3\rho C_p k^*} \frac{\partial^2 T}{\partial z^2} + \frac{q'''}{\rho C_p} \quad (10)$$

The corresponding boundary conditions are,

$$\begin{aligned} u = U_w = ax, v = V_w = by, w = 0, T = T_w, -D \frac{\partial C}{\partial z} = h_2 (C_w - C) \quad \text{at } z = 0 \\ u \rightarrow 0, v \rightarrow 0, T \rightarrow T_\infty, C \rightarrow C_\infty \quad \text{as } z \rightarrow \infty \end{aligned} \quad (11)$$

3. SOLUTION OF THE PROBLEM

The non-linear partial differential equations are transformed to the non-linear ordinary differential equations, with the assistance of following similarity transformations. $u = axf'(\eta), v = ayg'(\eta), w = -\sqrt{av}[f(\eta) + g(\eta)],$

$$\theta(\eta) = \frac{T - T_\infty}{T_w - T_\infty}, \phi(\eta) = \frac{C - C_\infty}{C_w - C_\infty}, \eta = \sqrt{\frac{a}{\nu}} z \quad (12)$$

Using (12), obviously satisfied the continuity equation (1), the Eqns. (2), (3), (5), (10) and related boundary conditions (11) are altered as follows.

$$(1 + \varepsilon) f''' - f'^2 + (f + g) f'' - \delta_1 \varepsilon f''^2 f''' - (M^2 + K) f' = 0 \quad (13)$$

$$(1 + \varepsilon) g''' - g'^2 + (f + g) g'' - \delta_2 \varepsilon g''^2 g''' - (M^2 + K) g' = 0 \quad (14)$$

$$(1 + R) \theta'' + \text{Pr}(f + g) \theta' + A^* f' + B^* \theta = 0 \quad (15)$$

$$\phi'' + \text{Sc}(f + g) \phi' - \text{KrSc} \phi = 0 \quad (16)$$

The corresponding non-dimensional boundary conditions are

$$\begin{aligned} f(0) = 0, g(0) = 0, f'(0) = 1, g'(0) = S, \theta(0) = 1, \phi'(0) = -\text{Bi}_2(1 - \phi(0)) \\ f'(\infty) \rightarrow 0, g'(\infty) \rightarrow 0, \theta(\infty) \rightarrow 0, \phi(\infty) \rightarrow 0 \end{aligned} \quad (17)$$

Here, the non-dimensional quantities are,

$$\varepsilon = \frac{1}{\mu\beta c}, \delta_1 = \frac{a^3 x^3}{2\nu c^2}, \delta_2 = \frac{a^3 y^3}{2\nu c^2}, M^2 = \frac{\sigma B_0^2}{a\rho}, K = \frac{\nu}{ak_p}, \text{Pr} = \frac{\mu C_p}{\kappa}, \text{Kr} = \frac{k_1}{a}, \text{Sc} = \frac{\nu}{D},$$

$$S = \frac{b}{a}, R = \frac{16\sigma^* T_\infty^3}{3\kappa k^*}, \text{So} = \frac{D_T K_T}{\nu T_m} \frac{(T_w - T_\infty)}{(C_w - C_\infty)}, \text{Bi}_2 = \frac{h_2}{D} \sqrt{\frac{\nu}{a}}$$

For practical and engineering point of view, the physical quantities like local skin friction along x and y -directions, local Nusselt and Sherwood numbers are considered in this chapter

$$Cf_x = \frac{\tau_{xz}}{\rho U_w^2}, Cf_y = \frac{\tau_{yz}}{\rho V_w^2}, Nu_x = \frac{xq_w}{\kappa(T_w - T_\infty)}, Sh_x = \frac{xj_w}{D(C_w - C_\infty)} \quad (18)$$

Here, τ_{xz} and τ_{yz} are the wall shear stresses along x and y -directions respectively, as follows

$$\tau_{xz} = \left(\mu + \frac{1}{\beta c} \right) \frac{\partial u}{\partial z} - \frac{1}{6\beta c^3} \left(\frac{\partial u}{\partial z} \right)^3, \quad \tau_{yz} = \left(\mu + \frac{1}{\beta c} \right) \frac{\partial v}{\partial z} - \frac{1}{6\beta c^3} \left(\frac{\partial v}{\partial z} \right)^3 \quad (19)$$

The heat and mass fluxes at the surface are given by

$$q_w = - \left[K + \frac{16\sigma^* T_\infty^3}{3k^*} \right] \left(\frac{\partial T}{\partial z} \right)_{z=0}, \quad j_w = -D \left(\frac{\partial C}{\partial z} \right)_{z=0} \quad (20)$$

These equations are transmuted into the following dimensionless forms

$$\text{Re}_x^{1/2} C f_x = (1 + \varepsilon) f'' - \frac{\delta_1 \varepsilon}{3} f''^3 \quad (21)$$

$$\text{Re}_y^{1/2} C f_y = (1 + \varepsilon) g'' - \frac{\delta_2 \varepsilon}{3} g''^3 \quad (22)$$

$$\text{Re}_x^{-1/2} Nu_x = -(1 + R) \theta'(0) \quad (23)$$

$$\text{Re}_x^{-1/2} Sh_x = -\phi'(0) \quad (24)$$

$$\text{Where, } \text{Re}_x = \frac{U_w x}{\nu} \text{ and } \text{Re}_y = \frac{V_w y}{\nu} \text{ are local Reynolds numbers.}$$

4. RESULTS AND DISCUSSION

The set of non-linear ordinary differential equations (13)-(16) with the boundary conditions (17) are solved numerical method along with MATLAB bvp4c by Shooting technique. If exist any variations between their corresponding values, the process continued until the required good values. Under the limited conditions $M = K = \varepsilon = \delta_1 = \delta_2 = 0$, presents results compared with the previously existed results of Hayat et al. [35] in

Table 1.

The effects of various flow parameters on velocity, temperature and species concentration have been presented graphically in Figs. 2-19. Also, presented the numerical values of skin friction coefficients, local Nusselt number and local Sherwood number in Tables 2 and 3. We have used the values $M = K = Kr = S = Bi_2 = 0.5$, $\varepsilon = \delta_1 = \delta_2 = R = So = 1, A^* = B^* = 0.2, Pr = 3$ and $Sc = 0.6$ throughout the present analysis.

From Fig.2 illustrated that the axial and transverse velocities are depreciated with application of strong magnetic field (M). Physically, the drag forces particularly Lorentz force generated with employing of magnetic field, these force opposed the flow of fluid hence both axial and transverse velocities are reduced. The magnetic field improves the internal friction in flow field, this friction causes to the increment of fluid temperature, it is observed from Fig.3. It is similar trend observed in specious concentration from Fig. 4. The effect of porosity parameter (K) on velocity, temperature and concentration streams is pictured in Figs.5 to 7. The axial and transverse velocities and momentum boundary layer thickness are reduced with enhancing of (K) this phenomenon observed in Fig.5. The thermal boundary layer thickness and fluid temperature are enhanced with (K) it is shown in Fig.6 behavior is observed in specious concentration from Fig.7. Basically, enhancing of porosity causes to high permeability of fluid hence maximum fluid permitted in normal direction it leads to decelerating of axial and transverse velocities.

Fig.8 shows the opposite tendency of axial and transverse velocities with the influence of stretching ratio parameter (S). In general S is the ratio between transverse and axial velocities, the increasing of (S) means that the transverse velocity dominates the axial velocity. The colder region intensity increased due to the stretching of the surface hence the fluid temperature reduced with increasing values of (S), and this phenomenon is shown in Fig. 9. Figs. 10-12 illustrate the influence of fluid parameter ε on velocity, temperature and concentration fields. It is noticed that the fluid velocity increases with an increase in (ε). So, the viscosity of fluid decreases. As a consequence, we notice

decay in the temperature and concentration fields with an increase in \mathcal{E} . The increment of Eyring-Powell fluid parameter (δ_1) causes to decelerating of axial velocity consequently increases the transverse velocity this phenomenon observed in Fig.13. The quite opposite tendency was noticed with rising of Eyring-Powell fluid parameter (δ_2) in axial and transverse velocities see Fig.14.

The thickness of thermal boundary layer and fluid temperature are enhanced with higher thermal radiation parameter (R) it is shown in Fig.15. Figs.16 and 17 demonstrate the influence of space and temperature dependent heat source or sink parameters on temperature profile. It reveals that the positively increasing values of A^* and B^* increases the fluid temperature and thickness of thermal boundary layer while negatively increasing values of A^* and B^* decreases the fluid temperature and thickness of thermal boundary layer. Generally, when $A^* > 0$ and $B^* > 0$ they plays a role of heat generators and produces more heat to fluid then the fluid temperature is increased. But in case $A^* < 0$ and $B^* < 0$ they acts the heat absorbents and absorbs heat from fluid then the fluid temperature is decreased.

Fig.19 illustrates the dimensionless concentration distribution for various values of chemical reaction parameter. It is evident that an increase in (Kr) depreciates the fluid concentration. Particularly, the high chemical reaction increases the interfacial mass transfer it causes to reducing of solutal boundary layer thickness and fluid concentration. The species concentration is decreased with rising values of thermal radiation parameter (R) this phenomenon is observed from Fig.20. The comparison of current results with the previous results of Hayat et al. [35] is tabulated in Table 1. From this table we conclude that our results are very good agreement with the existing results in some limiting cases. The numerical values of local skin friction factor coefficients at $z = 0$ (i.e., xy - plane) due to the velocity distributions on axial and transverse directions for various physical parameters are represented in Table 2. We observed that the magnetic field increases the local friction factors due to the reason that the Lorentz forces arises with magnetic field which creates internal friction. The increment of Eyring-Powell fluid parameter \mathcal{E} leads to increment in dynamic viscosity it causes to rising of local skin-friction. The similar tendency observed with growing of magnetic parameter (M), porosity parameter (K) and stretching ratio parameter (S). Moreover, local frictions retarded with rising of (δ_1) and (δ_2) since the respective velocities are declined with δ_1 and δ_2 .

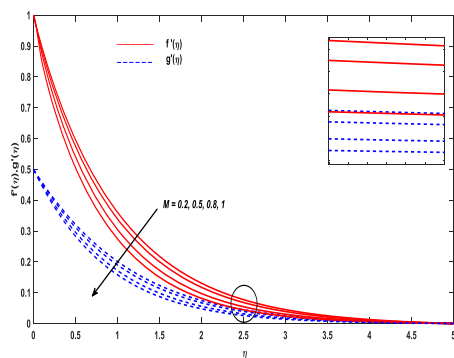


Fig.1. Effect of (M) on velocity

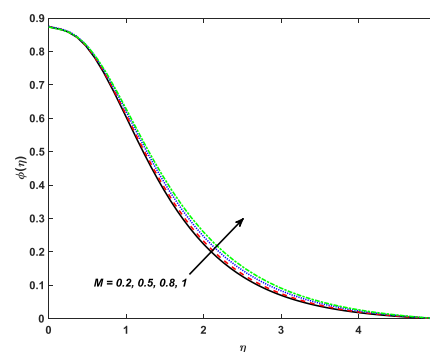


Fig.2. Effect of (M) on concentration

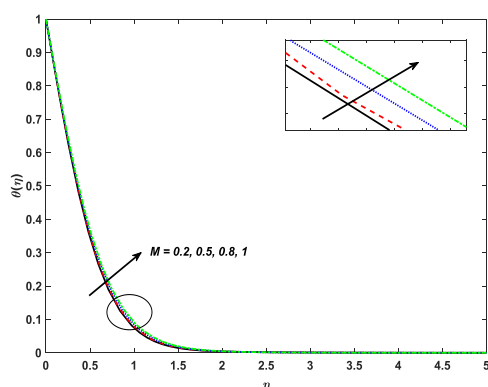


Fig.3. Effect of (M) on temperature

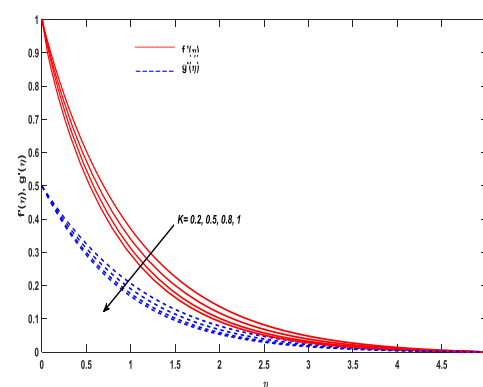


Fig.4. Effect of (K) on velocity

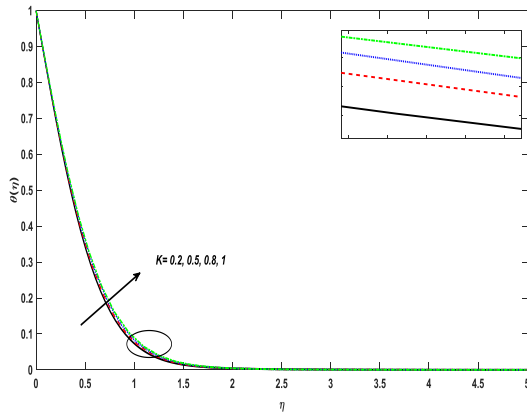


Fig.5. Effect of (κ) on temperature

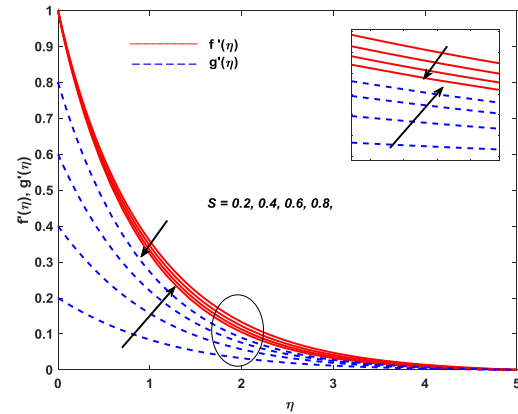


Fig.6 Effect of (s) on velocity

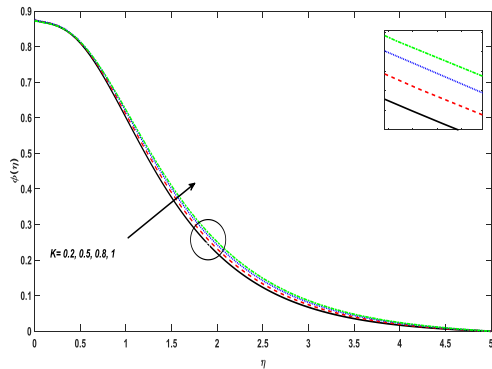


Fig.7. Effect of (κ) on concentration

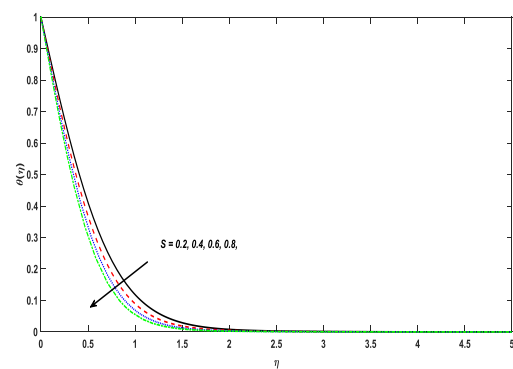


Fig.8. Effect of (s) on temperature

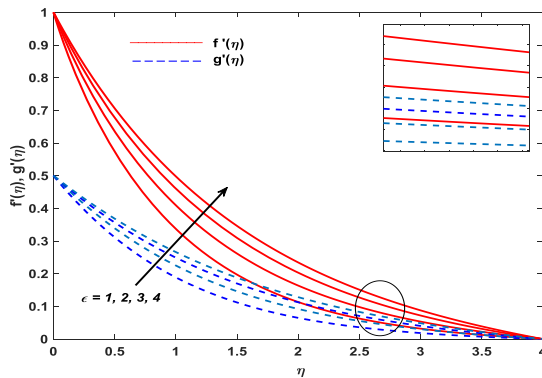


Fig.9. Effect of (ϵ) on velocity

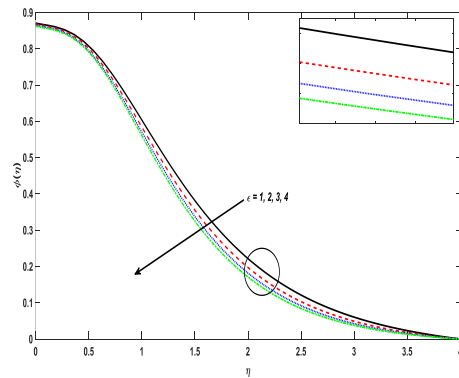


Fig.10 . Effect of (ϵ) on concentration

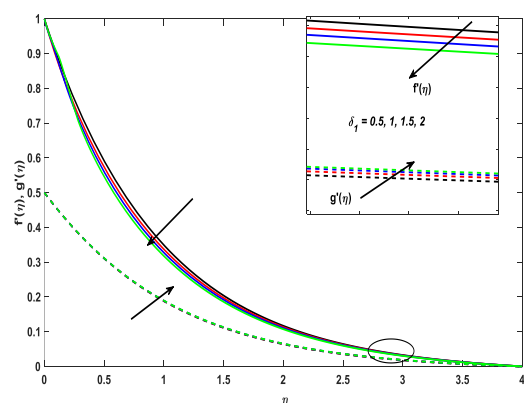
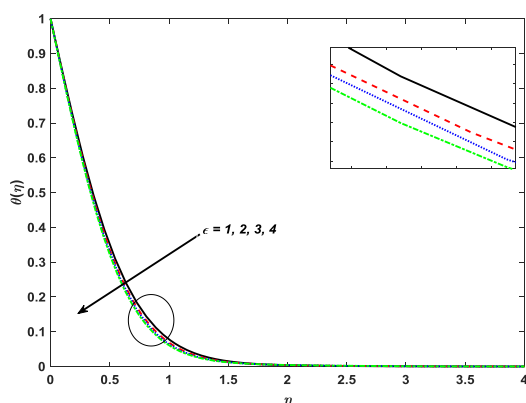


Fig.11. Effect of (ε) on temperature

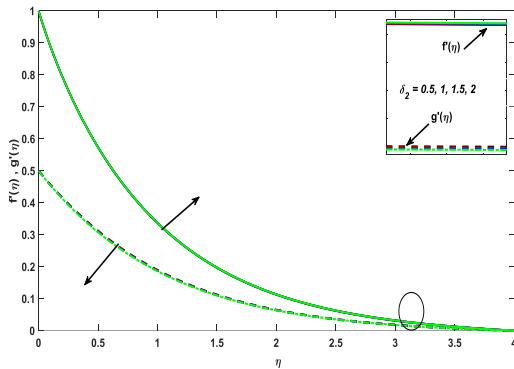


Fig.11. Effect of (δ_1) on velocity

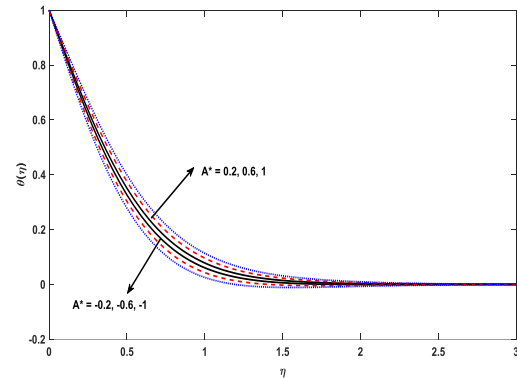


Fig.12. Effect of (δ_2) on velocity

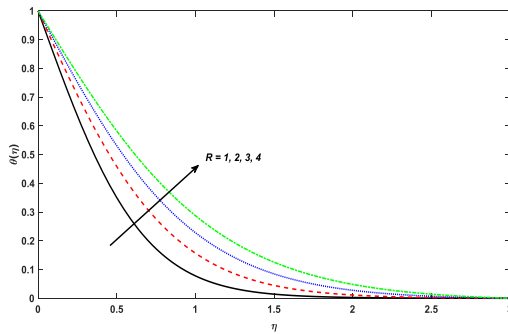


Fig.13. Effect of (A^*) on temperature

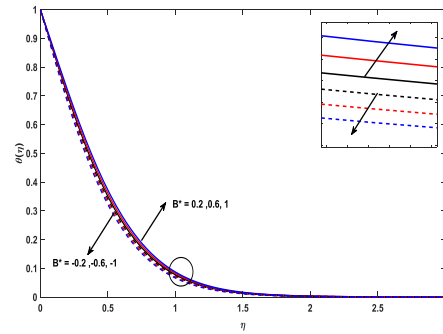


Fig.14. Effect of (R) on temperature

Fig.15. Effect of (B^*) on temperature

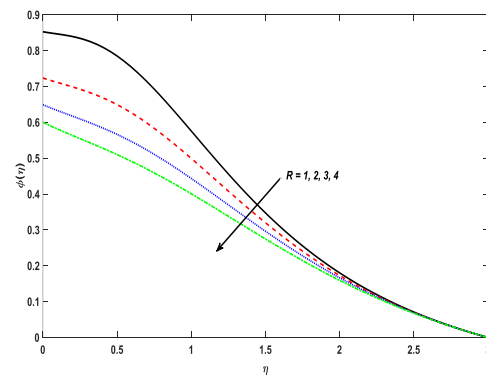
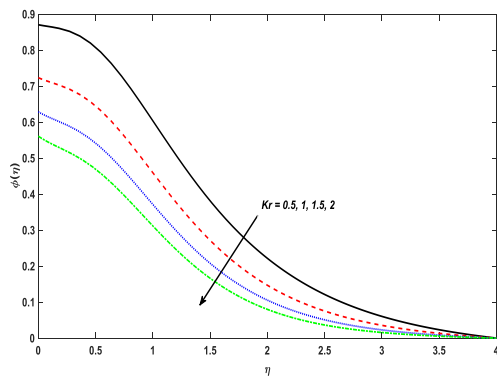


Fig.16. Effect of (K_r) on concentration

Fig.17. Effect of (R) on concentration

Table 1 : Comparison results for $-f''(0)$ and $-g''(0)$

S	$-f''(0)$		$-g''(0)$	
	Hayat et al. [35]	Present results	Hayat et al. [35]	Present results
0	1	1.000001	0	0
0.1	1.020260	1.020260	0.066847	0.066847
0.2	1.039495	1.039496	0.148737	0.148737
0.3	1.057955	1.057955	0.243359	0.243360
0.4	1.075788	1.075788	0.349209	0.349209

0.5	1.093095	1.093095	0.465205	0.465205
0.6	1.109947	1.109947	0.590529	0.590529
0.7	1.126398	1.126398	0.724532	0.724532
0.8	1.142489	1.142489	0.866683	0.866683
0.9	1.158255	1.158254	1.016540	1.016539
1	1.173722	1.173721	1.173722	1.173721

Table 2: Numerical values of local skin friction coefficients.

M	K	ε	S	δ_1	δ_2	$Cf_x Re_x^{1/2}$	$Cf_y Re_y^{1/2}$
0.1	0.5	1	0.5	1	1	1.769065	0.832016
0.3						1.801482	0.853211
0.5						1.862260	0.894290
	1					1.791876	0.957459
	1.5					1.871427	1.069951
		2				2.214923	1.044391
		3				2.626414	1.240166
			0.7			1.797209	1.229155
			0.9			1.822864	1.638329
				0.5		1.824480	0.833865
				1.5		1.537837	0.828541
					0.5	1.769255	0.835728
					1.5	1.768870	0.828159

5. CONCLUSIONS

The three-dimensional hydromagnetic flow of an Eyring-Powell non -Newtonian fluid on a bilinear stretching sheet embedded porous medium has been considered to investigate the thermal radiation , non-uniform heat source/sink and first ordered chemical reaction with the diffusion slip condition. The attained results are achieved to the natural phenomenon of Eyring-Powell fluid. The major outcomes of the present investigation are summarized below,

- The fluid velocities are boosts up with ε and opposite attitude noticed in temperature and specious concentrations distribution.
- The fluid temperature increases with enhancing of R .
- The specious concentrations increases with decreasing of Kr .
- The rising values of stretching ratio parameter increases the coefficients of local friction factors along axial and transverse directions.
- The rate of heat and mass transfers are enriched with ε and R .
- The specious concentrations are higher in presence of mass transfer Biot number γ .

Nomenclature

(x, y, z)	Velocity components	ν	Kinematic viscosity
μ	Dynamic viscosity coefficient	M	Magnetic field parameter
β, c	Eyring-Powell fluid characteristics	σ	Electric conductivity
ρ	Density of the fluid	K	Porosity parameter
$\varepsilon, \delta_1, \delta_2$	Eyring-Powell fluid parameters	k_p	Porous medium permeability

S	Stretching ratio parameter	R	Thermal radiation parameter
k^*	Mean absorption coefficient	α	Thermal diffusivity
(u, v, w)	Velocity components	C_p	Specific heat
Pr	Prandtl number	Sc	Schmidt number
σ^*	Stefan-Boltzmann constant	K_T	Thermal diffusion ratio
k_1	Reaction rate		

6. REFERENCES

- [1] M. Patel and M. G. Timol, Numerical treatment of Powell-Eyring fluid flow using method of satisfaction of asymptotic boundary conditions (MSABC), *Applied Numerical Mathematics*, 59 (2009) 2584–2592.
- [2] T. Hayat, M. Awais, and S. Asghar, Radiative effects in a three-dimensional flow of MD Eyring-Powell fluid, *J. Egy pt.Math. Soc.* 21 (2013) 379-384.
- [3] A. Ara, N. A. Khan, H. Khan, and F. Sultan, Radiation effect on boundary layer flow of an Eyring-Powell fluid over an exponentially shrinking sheet, *Ain-Shams Eng. J.* 5 (2014)1337-1342.
- [4] T.Javed, N. Ali, Z. Abbas, and M. Sajid, Flow of an Eyring-Powell Non-Newtonian fluid over a stretching sheet, *Chemical Engineering Communications*, 200 (2013) 327-336.
- [5] N.S. Akbar, S. Nadeem, Characteristics of heating scheme and mass transfer on the peristaltic flow for an Eyring-Powell fluid in an endoscope. *Int J Heat Mass Transfer*, 55 (2012) 375–383.
- [6] T. Hayat, Z. Iqbal, M. Qasim, S. Obidat, Steady flow of an Eyring Powell fluid over a moving surface with convective boundary conditions, *Int. J. Heat Mass Transf.*, 55 (2012)1817–1822.
- [7] A.V. Rosca, I.M. Pop, Flow and heat transfer of Powell-Eyring fluid over a shrinking surface in a parallel free stream, *Int. J.Heat Mass Transf.*, 71 (2014) 321–327.
- [8] M. Jalil, S. Asghar, S.M. Imran, Self similar solutions for the flow and heat transfer of Powell-Eyring fluid over a moving surface in a parallel free stream, *Int. J. Heat Mass Transf.*, 65 (2013) 73–79.
- [9] E. Magyari, M.E. Ali and B. Keller, Heat and mass transfer characteristics of the self-similar boundary layer flows induced by continuous surfaces stretched with rapidly decreasing velocities, *Heat and Mass Transfer*, 38 (2001) 65-74.
- [10] C.H. Chen, Combined Heat and mass transfer in MHD free convection from a vertical surface with Ohmic heating and viscous dissipation, *International Journal of Engineering Science*, 42 (2014) 699–713.
- [11] S.S. Sagar and G.K. Dubey, MHD free convection heat and mass transfer flow of viscoelastic fluid embedded in a porous medium of variable permeability with radiation effect and heat source in slip flow regime, *Advances in Applied Science Research*, 2 (2011) 115-129.
- [12] M. Patel, M.G. Timol, Numerical treatment of Powell-Eyring fluid flow using method of satisfaction of asymptotic boundary conditions (MSABC), *Appl. Numer. Math.* 59 (2009) 2584–2592.
- [13] B.J. Gireesha, G.M .Pavithra, C.S. Bagewadi, Boundary layer flow and heat transfer of a dusty fluid over an expo- nentially stretching sheet. *Br. J. Math.Comput. Sci.*, 2(4) (2012)187–97.
- [14] S. Mukhopadhyay, Slip effects on MHD boundary layer flow over an exponentially stretching sheet with suction/blowing and thermal radiation, *Ain Shams Eng. J.*, 4 (2013) 485–491.
- [15] M.Q. Al-Odat, R.A. Damesh, and T.A. Al-Azab, Thermal boundary layer on an exponentially stretching continuous surface in the presence of magnetic field, *Int. J. Appl. Mech. Eng.*, 11 (2006) 289-299.
- [16] M.Y. Malik, A. Hussain, S. Nadeem, Boundary layer flow of an Eyring-Powell model fluid due to a stretching cylinder with variable viscosity. *Scientia Iranica Mech Eng.*, 20(2) (2013) 313–321.
- [17] N.T.M. Eldabe S.N. Sallam, M.Y. Abou-zeid, Numerical study of viscous dissipation effect on free convection heat and mass transfer of MHD non-Newtonian fluid flow through a porous medium. *J Egy Math Soc .*, 20 (2012)139–151.
- [18] K. Rubab and M. Mustafa, Cattaneo-Christov heat flux model for MHD three Dimensional flow of maxwell fluid over a stretching sheet,*PLOS ONE*, 11 (2016) 1-16.
- [19] S.M. Murshed, C.A. Nieto de Castro, M.J.V. Lourenço, M.L.M. Lopes and F.J.V. Santos, A review of boiling and convective heat transfer with nanofluids, *Renewable and Sustainable Energy Reviews*, 15 (2011) 2342-2354.

- [20] A.K. Najeeb, A. Shahnaila and A.K. Nadeem, MHD flow of Powell–Eyring fluid over a rotating disk, *Journal of the Taiwan Institute of Chemical Engineers*, 45 (2014) 2859-2867.
- [21] M. Y. Malik, I. Khan, A. Hussain and T. Salahuddin, Mixed convection flow of MHD Eyring-Powell nanofluid over a stretching sheet: A numerical study, *AIP ADVANCES*, (2015) 1-13.
- [22] B. Mahanthesh, B.J. Gireesha, G. Rama Subba Reddy, Unsteady three-dimensional MHD flow of a nano Eyring-Powell fluid past a convectively heated stretching sheet in the presence of thermal radiation, viscous dissipation and Joule heating, *Journal of the Association of Arab Universities for Basic and Applied Sciences*, 23 (2017) 75–84.
- [23] T. Hayat, R. Sajjad, T. Muhammad, A. Alsaedi and R. Ellahi, On MHD nonlinear stretching flow of Powell–Eyring nanomaterial, *Results in Physics*, 7 (2017) 535–54.
- [24] T.Hayat, M.I. Khan and M.Waqas, Effectiveness of magnetic nanoparticles in radiative flow of Eyring-Powell fluid, *Journal of Molecular Liquids*, 231 (2017) 126-133.
- [25] S. Han, L. Zheng and C. Li, X. Zhang, Coupled flow and heat transfer in viscoelastic fluid with Cattaneo-Christov heat flux model, *Applied Mathematics Letters*, 38 (2014) 87–93.
- [26] T.Hayat, M.Imtiaz, and A.Alsaedi, Effects of homogeneous-heterogeneous reactions in flow of Powell-Eyring fluid, *Journal of Central South University*, 22 (2015) 3211-3216.
- [27] J. Rahimi , D.D. Ganji, M. Khaki and K. Hosseinzadeh, Solution of the boundary layer flow of an Eyring-Powell non-Newtonian fluid over a linear stretching sheet by collocation method, *Alexandria Engineering Journal*, 56 (2017) 621-627.
- [28] S. Geethan Kumar, S.V.K. Varma and P. Durga Prasad, Diffusion-Thermo effect on three-dimensional conducting flow of Eyring-Powell fluid over a bilinear stretching porous sheet with chemical reaction and diffusion slip, *Advanced Science Engineering and Medicine*, 10 (2018) 1205-1211.
- [29] A. Ishak, K. Jafar, R. Nazar and I. Pop, MHD stagnation point flow towards a stretching sheet, *Physica A: Statistical Mechanics and its Applications*, 388 (2009) 3377–3383.
- [30] A. Dawar, Z. Shah, M. Idrees, W. Khan, S. Islam and T. Gul, Impact of thermal radiation and heat source/sink on Eyring-Powell fluid flow over an unsteady oscillatory porous stretching surface, *Mathematical and Computational Applications*, 23 (2018) 1-18.
- [31] J.A. Gbadeyan, A.S. Idowu, A.W. Ogunsola, O.O. Agboola and P.O.Olanrewaju, Heat and mass transfer for Soret and Dufour’s effect on mixed convection boundary layer flow over a stretching vertical surface in a porous medium filled with a viscoelastic fluid in the presence of magnetic field, *Global Journal of Science Frontier Research*, 11 (2011) 1-19.
- [32] N.A. Khan , S. Aziz and S. Ullah, Entropy generation on MHD flow of Powell-Eyring fluid between radially stretching rotating disk with diffusion-thermo and thermo-diffusion effects, *Acta Mechanica et Automatica*, 11 (2017) 20-32.
- [33] M. Suali, N.M.A. Nik Long and A. Ishak, Unsteady stagnation point flow and heat transfer over a stretching/shrinking sheet with prescribed surface heat flux. *Applied Mathematics and Computational Intelligence*, 1 (2012) 1-11.
- [34] H. Zaman, M.A. Shah and M.Ibrahim, Unsteady incompressible Couette flow problem for the Eyring-Powell model with porous walls, *American Journal of Computational Mathematics*, 3 (2013) 313-32.
- [35] T. Hayat, I. Ullah, T. Muhammad, A. Alsaedi and S.A. Shehzad, Three-dimensional flow of Powell-Eyring nanofluid with heat and mass flux boundary conditions, *Chin J Phys*, 25 (2016) 1-9.